Proc. Natl. Acad. Sci. USA
Vol. 83, pp. 649–653, February 1986
Biophysics

The nature of enzyme catalysis in trypsin

S. J. WEINER, G. L. SEIBEL, AND P. A. KOLLMAN

Department of Pharmaceutical Chemistry, School of Pharmacy, University of California, San Francisco, CA 94143

Communicated by Walther Stoeckenius, August 26, 1985

ABSTRACT **We present a combined quantum/molecular mechanical study of the trypsin-catalyzed hydrolysis of a specific tripeptide substrate, including the entire enzyme in the calculation, as well as 200 H_2O molecules. The results illustrate how the enzyme and nearby H_2O molecules stabilize the ionic intermediates in peptide hydrolysis, such that the reaction is calculated to have a barrier that is significantly smaller than the calculated and experimental base-catalyzed barrier of formamide hydrolysis in aqueous solution. This enables us to understand how serine proteases increase the rates for reactions that take place in their active sites, compared to the corresponding rates for analogous solution reactions.**

One of the most interesting challenges faced by the theoretical biophysical chemist is to simulate chemical reactions in enzyme active sites and compare these with corresponding reactions in solution. There have been a number of different approaches to such a problem (1–6) but, to our knowledge, none in which a detailed comparison of solution and enzymatic-catalyzed reactions have been carried out using a combination of *ab initio* quantum mechanics and molecular mechanics, including the entire enzyme, substrate, and a substantial number of explicit water molecules in the molecular mechanical model. We have recently developed an approach to include solvation and bond formation energies in simulations of complex systems and have applied it to gas phase and aqueous solution amide hydrolysis (7).

Trypsin was chosen as the model serine protease because its structure was known to high precision (8), there was much experimental kinetic data (9, 10) on the reactions it catalyzed, and it had a well-defined mechanism that was consistent with many structural and kinetic studies. Pozsgay *et al.* (10) found that the substrate Ac-Phe-Val-Lys(Me) possessed a higher catalytic efficiency than nearly all of other model tripeptides ($k_{cat}/K_m = 4.5 \times 10^4$/M·sec). For this reason, we selected this tripeptide (denoted Sub) for study. Below, we simulate amide bond cleavage in the active site of a serine protease and compare the reaction profiles for gas-phase, aqueous-phase, and enzyme-catalyzed peptide hydrolysis.

METHODS

The proteolysis of peptides catalyzed by trypsin is thought to occur as described in Scheme 1, in which the depicted structures are representations of the calculated structures considered here. Structure (*A*) represents the Michaelis complex KM. The serine proton is transferred to histidine to form structure KMION (*B*). The serine O_γ substrate carbonyl bond begins to form with a distance of 2.08 Å [208 structure (*C*)] and then this bond is ≈1.48 Å in the tetrahedral intermediate [TET1 structure (*D*)]. The histidine delivers back the proton to the leaving group NHR on the substrate (*E*) (structure 115, in which the H···N distance is 1.15 Å and the amide bond C···N 1.75 Å). After this bond has been totally cleaved, a water molecule forms a hydrogen bond to the histidine [structure ACYLWAT (*F*)], and then transfers its proton as it attacks the acylenzyme to form the second tetrahedral intermediate [structure TET2 (*G*)], which then breaks down by proton transfer from histidine to the serine O_γ to regenerate the native enzyme.

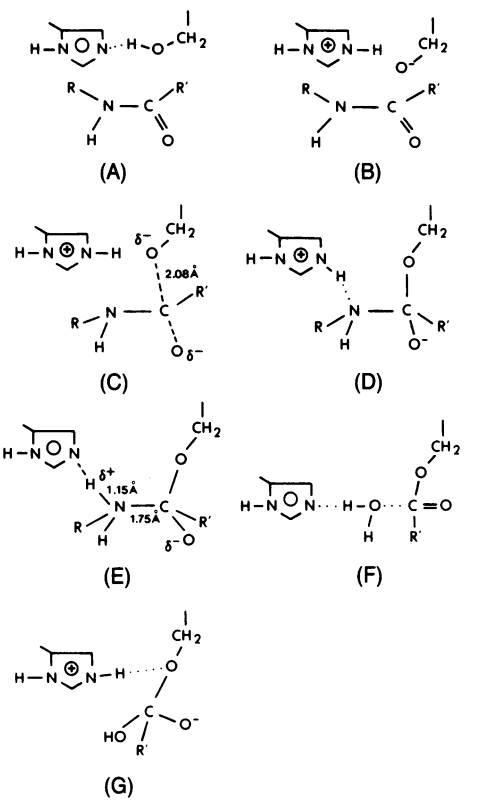

Each model-built structure consists of the entire trypsin molecule [taken from the x-ray crystal structure of Chambers and Stroud (8) (resolution 1.5 Å)]. Each complex also contains 200 explicit water molecules. Of these 200, 100 of the oxygen positions were taken from the work of Chambers and Stroud and the neutron diffraction study by A. Kossiakoff (personal communication). These water molecules were selected if the water oxygen was less than 3.4 Å from any two atoms in trypsin. The hydrogen atomic positions were then placed manually, maximizing hydrogen-bonding potential with both protein and neighboring water structure.

To model SUB into the active site of trypsin we used structural information from the x-ray crystal structure of trypsin/bovine pancreas trypsin inhibitor (11), attempting to form analogous H bonds.

The next step was to take the trypsin/Sub/100 "tightest" interacting water molecules and to immerse them into a "giant" cube of water. This "giant" cube was generated by taking a single snapshot from a Monte Carlo simulation performed on a

The publication costs of this article were defrayed in part by page charge payment. This article must therefore be hereby marked "*advertisement*" in accordance with 18 U.S.C. §1734 solely to indicate this fact.

Abbreviations: Sub, Ac-Phe-Val-Lys(Me); MP2, Moller–Plesset second-order perturbation theory; SCF, self-consistent field.

cube of 216 water molecules (12) and translating it in the $\pm x$, $\pm y$, and $\pm z$ directions to form a "giant" cube (27 cubes of 216 water molecules each). We then used software within the computer program AMBER (13, *) to select those water molecules within 15 Å of the active site scissile bond and that were not within 2.35 Å of any Kossiakoff/Stroud trypsin or water atom. This lead to a continuous water structure about the active site and a system consisting of native trypsin (residues 1–223), Sub (residues 224–228), 100 Kossiakoff/Stroud H_2O (residues 229–328), and 100 H_2O added by AMBER (residues 329–428).

At this point, there were several close water protein and water–water interaction distances, which we removed by keeping trypsin fixed and allowing the entire water structure to energy refine about the enzyme for 100 cycles of steepest descent minimization. This model of trypsin/Sub/100 Kossiakoff/Stroud H_2O (relaxed)/100 AMBER H_2O (relaxed) was used as the starting structure of the KM complex and taken as the basis for the other complexes.

As the reactive serine-195 O_γ^- attacks the carbonyl carbon center, the peptide bond to be cleaved lengthens, and the peptide linkage carbon and nitrogen atoms begin to take on more sp^3 character. To best incorporate this into the molecular mechanics model, we have used quantum mechanically optimized geometries from earlier *ab initio* calculations on formamide hydrolysis by hydroxide ion (7). The formamide molecule is analogous to the peptide linkage to be cleaved while the OH^- is representative of the attacking serine-195 O_γ^-. To force structures 208, TET1, 115, and TET2 to mimic analogous structures found in the formamide/OH^- study, we have used large bond and angle force constants (K_r = 5000 kcal/Å^2 and K_θ = 1000 kcal/rad^2; 1 cal = 4.184J) and appropriate equilibrium bond and angle values about these groups in the molecular mechanics model. In our energy refinement, we have employed a distance based and an explicit "residue-by-residue" based cutoff for selecting the nonbonded interaction pairs. Any residue or water molecule that had at least one atom within 10 Å of the reactive serine-195 was included in the "active site" model of the protein, and the rest of the atoms were held fixed. For the active site model, we then used a residue based distance cutoff of 8 Å [i.e., nonbonded interactions were calculated for any residue (or water molecule) that had at least one atom within 8 Å of any active site atom]. This corresponded to ≈165,000 nonbonded pair interactions, which enabled us to carry out a molecular mechanical minimization to a rms gradient of <0.1 kcal/mol·Å in about 20 min of central processing unit time on a Cray X-MP computer (typically 3000–5000 energy evaluations were required). Because our model included waters explicitly, we used a dielectric constant = 1 throughout, the force field parameters for the protein atoms from Weiner *et al.* (14), and the TIPS3P (12) for the water.

Ab initio quantum mechanical energies of the important active site atoms were calculated using Gaussian 82.† The calculations were performed with a 4-31G basis set (15) at the self-consistent field (SCF) and Moller–Plesset second-order perturbation theory (MP2) (16) levels. Each SCF and MP2 calculation took 1.5–2 hr on the Cray X-MP computer. For the steps leading up to the acylenzyme, this model consisted of imidazole (or imidazolium), methanol (or methoxide ion), and formamide; with the key heavy atom positions coming from the energy refined coordinates of histidine-57, serine-195, and the Sub backbone. For the ACYLWAT and TET2 geometries, our quantum mechanical model consisted of imidazole (or imidazolium), water (or attacking hydroxide), and methyl formate. All hydrogen atoms not included in the molecular mechanics model were added with standard bond lengths and bond angles.

After energy refining the various structures, the net molecular mechanical energy was evaluated by partitioning the system into five groups: (*i*) the atoms that are in the quantum mechanical model, (*ii*) the remainder of the substrate, (*iii*) the protein residues that have any atom within 8.5 Å of any quantum mechanical atom, (*iv*) the water molecules that have an atom within 8.5 Å of any quantum mechanical atom, and (*v*) the rest of the protein and water molecules. Since group (*i*) is included in the quantum mechanical model, we do not use its molecular mechanical energy. Rather, we evaluate the molecular mechanical energy reported in Table 1 by using the AMBER (13, †) energy analysis program and evaluating the internal energy of groups (*ii–iv*) and their interactions with each other and with group (*i*), the quantum mechanical atoms.

The molecular mechanics refinement and *ab initio* quantum mechanical calculations were carried out at Cray Research, Inc. in Mendota Heights, MN. All of the structures were model built and analyzed visually on the Evans and Sutherland PS2 computer using the program MIDAS§ in the Computer Graphics Laboratory at the University of California at San Francisco.

RESULTS

In Table 1, we report the energies for the individual steps of the catalytic reaction, with the *ab initio* quantum mechanical energies reported at the SCF and MP2 levels. One can see from the reported energies that the reaction profile for the enzyme catalyzed reaction is predicted to be remarkably flat, with the relative destabilization relative to the Michaelis complex calculated quantum mechanically almost exactly balanced by the stabilization of the system due to nonbonded (molecular mechanical) interactions. This stabilization comes mainly from electrostatic interactions, since the tetrahedral intermediate for serine protease catalysis is a zwitterion (*iv*) and the Michaelis complex (*i*) is neutral.

We present stereoviews of most of the structures in Fig. 1. It is clear from crystallographic studies that a good hydrogen

*Singh, U. C., Weiner, P. & Kollman, P. (1984) AMBER (University of California, San Francisco).

†Binkley, S. & Pople, J. A. (1982) Gaussian 82 (Carnegie–Mellon University, Pittsburgh, PA).

§Huang, C., Gallo, L., Ferrin, T. & Langridge, R. (1984) MIDAS (Computer Graphics Laboratory, University of California, San Francisco).

Table 1. Quantum and molecular mechanical energies of structures along the trypsin catalytic pathway

Structure	Quantum mechanical energy, kcal/mol MP2*	Quantum mechanical energy, kcal/mol SCF†	Molecular mechanical energy,‡ kcal/mol	Total energy,§ kcal/mol
KM	0	0	0	0
KMION	51.7	51.8	−68.3 (−57.2)	−16.6 (−5.5)
208	60.3	64.6	−57.7 (−57.5)	2.6 (2.8)
TET1	68.9	67.5	−64.0 (−61.6)	4.9 (7.3)
115	29.6	26.1	−21.6 (−20.5)	8.0 (9.1)
ACYLWAT	0	0	0	0
TET2	51.6	44.7	−59.2 (−55.4)	−7.6 (−3.8)

Values in parentheses represent energies if water-384 is not included in the calculations.

*Total energy of KM = −509.05805 atomic units (a.u.), ACYLWAT = −528.87813 a.u. using MP2 (17, 18).

†Total energy of KM = −508.02261 a.u., ACYLWAT = −527.82089 a.u. at the SCF level.

‡Energy relative to KM and ACYLWAT structure.

§Sum of MP2 quantum mechanical and molecular mechanical energies.

bond between histidine and serine is not formed in the native structures of the mammalian or bacterial serine proteases (19). However, an excellent Ser···His hydrogen bond is seen in the refined coordinates of trypsin/bovine pancreas trypsin inhibitor (11), a Michaelis complex analog. This H bond was model built into our KM structure (Fig. 1*A*), and it remained during minimization. The serine proton was transferred to histidine-57 to form the KMION structure (Fig. 1*B*). This structure is characterized by a similar Ser O_γ to carbonyl C distance (≈2.9 Å) as KM, but there are a number of interactions which strongly stabilize it, including two water H bonds, which interact strongly with the anionic serine O_γ. Both of these water molecules are modeled rather than actually located by neutron diffraction, and in particular one does not know whether water-384, which is "inside" the active site, is really there during trypsin catalysis. In fact, this water molecule has an interaction energy with its surroundings of only −11.6 kcal/mol in the KM structure, considerably less than the calculated energy of a water molecule in water (10) of −24.2 kcal/mol, whereas the other water molecules in the vicinity have much more favorable interaction energies. Thus, we have also evaluated the molecular mechanical energies with water-384 not included (Table 1). The main effect of the exclusion of water-384 is to make the relative energy of the KMION structure more realistic.

Structures 208 and TET1 (Fig. 1*C*) show the movement of the serine O_γ and its bond formation with the carbonyl carbon of the substrate. There are a number of interactions that stabilize TET1 over KM. The single most important is the hydrogen bond is found between the donor HN_δ of histidine-57 and one of the acceptor oxygen atoms of the aspartic acid COO^-. It is not surprising that the strongest hydrogen bond is formed for the tetrahedral complexes (TET1 and TET2), with hydrogen bond distances of 1.68 Å and 1.64 Å, respectively.

A second important interaction is that between the substrate and carbonyl oxygen and the oxyanion hole, which is defined by the two backbone hydrogens of glycine-193 and serine-195. The best hydrogen bonding structure is found for the tetrahedral intermediate structures; in TET1 two hydrogen bonds of 1.74 Å and 1.76 Å are formed between the carbonyl O^- and the backbone hydrogens. These N-H···O^- interactions are stronger in the TET1 structure than in the KM structure by a total of 11.5 kcal/mol. This differential stabilization can be related to the lower enzymatic activity (10^{-4} to 10^{-7}) of serine protease zymogens compared to the active enzymes (19). The crystal structure of trypsinogen does not have a properly oriented oxyanion hole (19). It is worth noting that a reduction by half of the oxyanion hole stabilization of the TET1 structure by the KM complex ($\Delta\Delta E^\ddagger$ = 5.8 kcal/mol) would correspond to reduction in rate of 10^{-4} if the tetrahedral complex formation was rate limiting in catalysis.

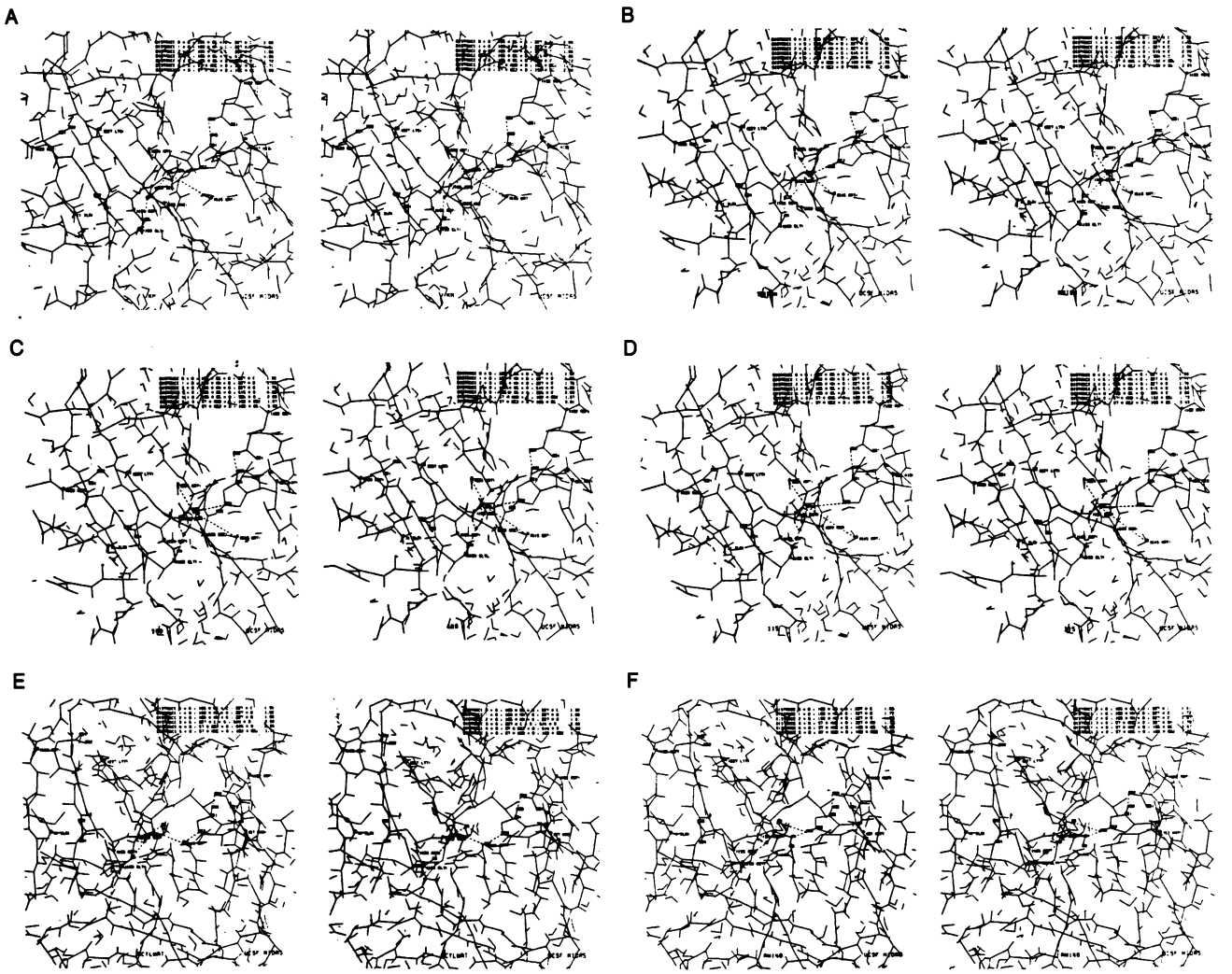

FIG. 1. Stereoviews of active site parts of various structures. Only the backbone atoms C, N, O, HN of many of the residues are shown, and the picture is clipped to highlight the active site region. The key residues are numbered according to the corresponding numbers in α-chymotrypsin. (*A*) KM structure. (*B*) KMION structure. (*C*) TET1 structure. (*D*) 115 structure. (*E*) ACYLWAT structure. (*F*) TET2 structure.

The third important active site interaction involves the hydrogen bonding of the lysine side chain in the specificity binding pocket to aspartic acid-189. This ion-pair interaction is very large in magnitude ($\Delta E \approx -90$ kcal/mol throughout the reaction), but is slightly weaker (by 4.3 kcal/mol) in the TET1 structure than in the KM complex and 3.0 kcal/mol weaker in the TET2 structure than in the ACYLWAT structure.

A fourth important interaction in trypsin is that between the salt bridge NH_2-terminal $NH_3^+ \cdots {}^-OOC$ aspartic acid-194 and the active site atoms and substrate. This interaction stabilizes the TET1 structure over the KM structure by 7.6 kcal/mol.

A final important stabilization of the TET1 structure over the KM structure is afforded by the water interactions, which stabilize the TET1 structure over the KM structure by 14.2 kcal/mol. This stabilization does not come predominantly from the closest waters and can be thought of as a reaction field stabilization of an ion pair in a partially aqueous environment.

The sum of the above interactions stabilize the TET1 structure over the KM structure by 57.6 kcal/mol, close to the total molecular mechanical stabilization of 64.0 kcal/mol noted in Table 1. Without forcing any particular orientation of histidine-57 relative to the tetrahedral intermediate structure, the side chain of this residue has moved during the molecular mechanics optimization to a very good position to deliver the HN_ε to the $NH(CH_3)$ end group [$R(HN_\varepsilon \cdots N) = 2.2$ Å, $\theta(N_\varepsilon(N_\varepsilon - HN_\varepsilon \cdots N) = 150°$] and, thus, to facilitate C–N bond cleavage. From this position, the proton can be transferred to 1.15 Å from the nitrogen and the scissile bond C–N lengthened to 1.75 Å, which mimics the geometry of the analogous structure in formamide hydrolysis in aqueous solution. The energy refined structure with the above two distance constraints is shown in Fig. 1*D*. As noted in Table 1, this structure has a quantum mechanical destabilization relative to the KM structure much less than the KMION, 208, and TET1 structures, but a correspondingly smaller protein/water stabilization of the active site residues, thus leaving it similar in total energy to those structures.

After the cleavage of the terminal amide bond, the acyl enzyme is formed. We have modeled this structure by orienting a hydrogen of the water molecule closest to histidine-57 toward N_ε of this residue and energy refining to yield ACYLWAT (Fig. 1*E*). Since our quantum mechanical model has changed, and we have removed the terminal amide, we cannot compare the energy of this structure directly with the prior structures. However, based on the formamide-OH^- study (7), we expect the ACYLWAT structure to be lower in energy than the 115 structure. We have not carried out as detailed an analysis of the deacylation part of amide hydrolysis, but have evaluated the structure and energy of the tetrahedral intermediate for deacylation (TET2, Fig. 1*F*). Again, as in the acylation step, the energy of this structure is comparable to the ACYLWAT structure, due to the cancellation of quantum mechanical destabilization and molecular mechanical stabilization (Table 1). Fig. 2 compares the schematic representation of the calculated reaction energetics of amide hydrolyses in the enzyme, in the gas phase, and in solution.

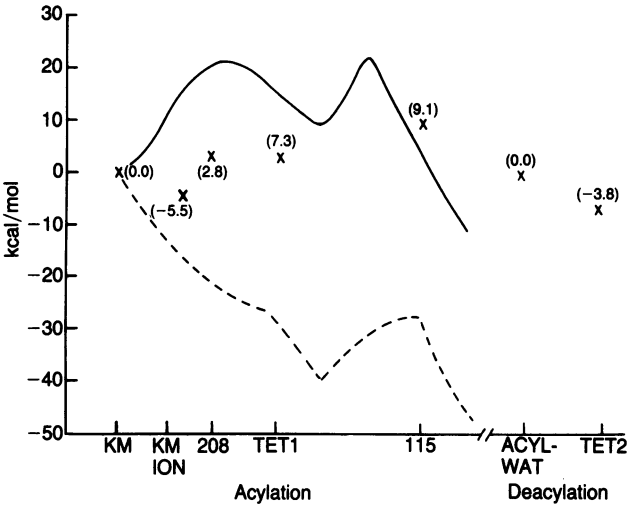

FIG. 2. Reaction profile for formamide hydrolysis in solution (—), in the gas phase (- - - -), and in the trypsin active site (×). Trypsin active site energies are taken from Table 1.

DISCUSSION AND CONCLUSIONS

We have examined the acylation step of amide hydrolysis in some detail and have simulated proton transfer from serine O_γ to histidine N_ε (KM to KMION), O_γ attack on the scissile carbonyl carbon (KMION to 208 to TET1), and proton transfer from the histidine back to the leaving group amine (TET1 to 115). As with any kinetic scheme, we cannot prove it correct. For example, serine to histidine proton transfer might be concerted with O_γ attack; however, we have found a nonconcerted process facile and would expect the barriers for an analogous concerted process to be even lower. We (6) and others (17, 18) have examined the energetics of proton transfer in detail and have concluded, that, as long as the atoms in the hydrogen bond are suitably oriented and are close enough together (<3.2 Å) and the two states (6) of proton transfer (A-H···B and $A^- \cdots$H-B^+) are similar in energy, the barrier to proton transfer should be in the range of 5–10 kcal/mol or less. The calculated structures and energies for serine to histidine and histidine-N (leaving group) proton transfer meet these criteria, so we expect that any other intermediate partially proton transferred structures will also be low in energy. Komiyama and Bender (20) have suggested that the proton transferred from serine-195 never fully reaches histidine-57 and, instead, veers off to the substrate amine, with its higher pK_a. We cannot rule out this possibility on the basis of the calculations reported here. However, it seems entropically unlikely (6, 17, 18) that all three groups (serine O_γ, histidine Nδ2 and substrate N) would be perfectly enough aligned to make such a single hop facile. Our calculations do show that a two step proton shuttle is very favorable.

The acylation step for amide hydrolysis is rate limiting, consistent with our calculated relative energies for the structures KM vs. TET1 (+7.3 kcal/mol) and ACYLWAT vs. TET2 (−3.8 kcal/mol). Two possible reasons for more rapid ester than amide hydrolysis in the enzyme are (*i*) the lower resonance energy of the ester than amide bond, reflected in the smaller quantum mechanical destabilization of structure TET2 compared to TET1 (Table 1) and (*ii*) the fact that, in the tetrahedral intermediate in amide hydrolysis (TET1), the leaving group nitrogen points its lone pair toward the histidine HN_ε, in order to form a stabilizing N-H···N hydrogen bond. Because of stereoelectronic effects (21) this conformation is higher by 3–5 kcal/mol than the one with the nitrogen inverted (7). In the case of an ester, one can orient a lone pair in the stereoelectronically favorable direction and still have the second lone pair pointing in the general direction of the histidine.

We have presented an approach for simulating an enzymatic reaction, incorporating the important internal and environmental energies. However, we note that our method can be improved. First, one could expand the active site quantum mechanical model, use a better basis set, and incorporate much of the external protein and solvent environment into the quantum mechanical calculation.

Second, we have used a dielectric constant of 1.0 in both the quantum and molecular mechanical models and a rela-

tively small nonbonded cutoff of 8 Å for evaluating nonbonded interactions.

Third, one of the largest uncertainties in the calculations is the location of water molecules, as we have noted above for water-384. Nonetheless, this water seems to artifactually stabilize only the most highly charged KMION structure (Table 1) with the remaining energies relatively unaffected.

Finally, we have not assessed the contribution of entropy to the reaction profile in order to assess free energies of enzyme catalysis (see, however, ref. 7).

Nonetheless, even with the large uncertainties in our calculated energies, discussed above, it is clear (Fig. 2) that the enzyme catalyzed reaction is quite different from the corresponding solution reaction and is part way between solution and gas phase profiles. In the enzyme active site, Michaelis complex, the O_γ is ≈3 Å from the carbonyl carbon with no water molecules in between. As the proton is delivered to the histidine N_ε, the waters in the active site, aspartic acid-102, the oxyanion hole, and the isoleucine-1-NH_3^+-aspartic acid-189 ion pair stabilize the ionic groups along the catalytic pathway, but, because these groups are mainly "preoriented" and fixed, little energy is required for this stabilization. Thus, our calculations give evidence for the fact that serine proteases achieve their efficiency over the corresponding solution reactions by both orienting the reacting groups and desolvating them during the binding step, prior to the formation of ionic structures. No desolvation of ionic structures is required, and the enzyme active site groups such as the oxyanion hole are preoriented during synthesis of the protein to stabilize such structures. In this paper we have not addressed the question of binding of substrate but that process involves releasing waters from the substrate and active site and derives its favorable free energy, as do most noncovalent protein–ligand interactions, by dispersion interactions, hydrophobic effects (release of water) and electrostatic complementarity (22). The significant catalytic enhancements achieved by biomimetic organic models (23, 24) of ester and amide hydrolysis can be rationalized on the basis of the orientation and desolvation effects noted above.

If histidine to amine proton transfer is the rate limiting step in trypsin catalysis, it is not likely to be because of the reason suggested by Huber and Bode (25). They suggested that since the histidine to amine distance is 4.2 Å in the trypsin/bovine pancreas trypsin inhibitor complex, a rate limiting conformational charge of histidine occurs during catalysis. Our calculations are consistent with our earlier calculations (26) on α-chymotrypsin with a different substrate in that during the formation of the tetrahedral intermediate, the histidine N_ε has moved to a good H bond position relative to the amine during the molecular mechanical optimization, with no barrier to this process. Our calculations are, unfortunately, not accurate enough to establish the serine to histidine proton transfer as the rate limiting step in trypsin catalysis of amides, but this remains the most likely possibility.

Warshel and Russell (27) have presented the results of calculations on structures like our KM, KMION, and TET1 using an empirical valence bond approach and a dipolar solvent model. Their solvation model is capable of more accurately reproducing pK_a values for enzyme groups than ours, but it is hard to evaluate the accuracy of the quantum mechanical approach they use. Dewar and Storch (28) have recently suggested that enzyme reactions are gas phase-like and have analyzed the serine protease mechanism on this basis. Although we disagree with their suggestion that histidine to aspartic acid proton transfer accompanies serine to histidine proton transfer (29), we agree with their suggestion that some desolvation is important in enzyme catalysis.

The recent and exciting results reported by Craik *et al.* (30), in which genetic engineering has been used to study trypsin catalysis in mutant enzymes provide important data to further assess calculations such as reported here. They found that glycine-216 to alanine and glycine-226 to alanine caused significant decreases in enzyme catalytic rates, as well as altering lysine/arginine specificities. By evaluating the relative quantum mechanical and molecular energies for the KM and TET1 structures in the mutant enzymes and for different substrates, the molecular mechanical approach presented here supplemented by free energy perturbation molecular dynamics methods (31) should enable one to assess how the two glycine to alanine substitutions destabilize the KM and TET1 structures and how this differs for lysine and arginine substrates.

We acknowledge the Institute of General Medical Sciences (GM-29072 to P.A.K.), the Division of Research Resources (RR-1081 to R. Langridge and the Computer Graphics Laboratory, University of California, San Francisco), and Cray Research, Inc. (Mendota Heights, MN) for research support.

1. Warshel, A. & Levitt, M. (1976) *J. Mol. Biol.* **103**, 227–249.
2. Bolis, G., Ragazzi, M., Salvadenri, D., Ferro, D. & Clementi, E. (1978) *Gazz. Chim. Ital.* **108**, 425–443.
3. Van Duijnen, P., Thole, B. & Hol, W. (1979) *Biophys. Chem.* **9**, 273–280.
4. Allen, L. C. (1981) *Ann. N.Y. Acad. Sci.* **367**, 383–406.
5. Umeyama, H., Hirono, S. & Nakagawa, S. (1984) *Proc. Natl. Acad. Sci. USA* **81**, 6266–6270.
6. Alagona, G., Desmeules, P., Ghio, C. & Kollman, P. (1984) *J. Am. Chem. Soc.* **106**, 3623–3632.
7. Weiner, S., Singh, U. C. & Kollman, P. (1985) *J. Am. Chem. Soc.* **107**, 2219–2229.
8. Chambers, J. & Stroud, R. (1977) *Acta Crystallogr., Sect. B.* **33**, 1824–1833.
9. Kraut, J. (1977) *Annu. Rev. Biochem.* **46**, 331–358.
10. Pozsgay, M., Szabo, G., Bajusz, S., Simonsson, R., Caspar, R. & Elodi, P. (1981) *Eur. J. Biochem.* **115**, 497–502.
11. Huber, R., Kukla, D., Bode, W., Schwager, P., Bartels, K., Deisenhofer, J. & Steigemann, W. (1974) *J. Mol. Biol.* **89**, 73–101.
12. Jorgensen, W., Chandresekhar, J. & Madura, J. (1983) *J. Chem. Phys.* **79**, 926–935.
13. Weiner, P. & Kollman, P. (1981) *J. Comp. Chem.* **2**, 287–303.
14. Weiner, S. J., Kollman, P., Case, D. A., Singh, U. C., Ghio, C., Alagona, G., Profeta, S. & Weiner, P. (1984) *J. Am. Chem. Soc.* **106**, 765–784.
15. Ditchfield, R., Hehre, W. & Pople, J. (1970) *J. Chem. Phys.* **52**, 5001–5007.
16. Binkley, J. & Pople, J. (1976) *Int. J. Quantum Chem.* **9**, 229–245.
17. Scheiner, S. & Harding, L. (1981) *J. Am. Chem. Soc.* **103**, 2169–2173.
18. Scheiner, S. & Hillebrand, E. (1985) *Proc. Natl. Acad. Sci. USA* **82**, 2741–2745.
19. Steitz, T. A. & Shulman, R. G. (1982) *Annu. Rev. Biophys. Bioeng.* **11**, 419–444.
20. Komiyama, M. & Bender, M. (1979) *Proc. Natl. Acad. Sci. USA* **76**, 557–560.
21. Lehn, J. & Wipff, G. (1980) *J. Am. Chem. Soc.* **102**, 1347–1354.
22. Kollman, P. (1984) in *X-Ray Crystallography and Drug Design*, eds. Horn, A. & C. De Ranter (Clarendon Press, Oxford, UK), pp. 63–82.
23. Rogers, G. & Bruice, T. (1974) *J. Am. Chem. Soc.* **96**, 2463–2488.
24. Page, M., ed. (1984) *The Chemistry of Enzyme Action* (Elsevier, Amsterdam), Chapters 14 and 15.
25. Huber, R. & Bode, W. (1978) *Acc. Chem. Res.* **11**, 114–122.
26. Wipff, G., Dearing, A., Weiner, P., Blaney, J. & Kollman, P. (1983) *J. Am. Chem. Soc.* **105**, 997–1005.
27. Warshel, A. & Russell, S. (1984) *Q. Rev. Biophys.* **17**, 283–423.
28. Dewar, M. & Storch, D. (1985) *Proc. Natl. Acad. Sci. USA* **82**, 2225–2229.
29. Hayes, D. M. & Kollman, P. A. (1981) *J. Am. Chem. Soc.* **103**, 2955–2961.
30. Craik, C., Largman, C., Fletcher, T., Roczmak, S., Barr, P., Fletterick, R. & Rutter, W. (1985) *Science* **228**, 291–297.
31. Postma, J. P. M., Berendsen, H. J. C. & Haak, J. R. (1982) *Faraday Symp. Chem. Soc.* **17**, 55–62.